A modern and powerful electrochemical sensing platform for purines determination: Voltammetric determination of uric acid and caffeine in biological samples on miniaturized thick-film boron-doped diamond electrode

Olha Sarakhman, Alžbeta Benková, Ľubomír Švorc *

Institute of Analytical Chemistry, Faculty of Chemical and Food Technology, Slovak University of Technology in Bratislava, Radlinského 9, Bratislava SK-812 37, Slovak Republic

ARTICLE INFO

ABSTRACT

In this study, an unmodified and powerful electrochemical sensor was introduced for the first time for the voltammetric determination of purine derivatives uric acid (UA) and caffeine (CAF). The miniaturized thick-film boron-doped diamond (BDD) electrode in tandem with cyclic voltammetry (CV) revealed two irreversible oxidation peaks at + 0.7 V and + 1.5 V for UA and CAF, respectively, in Britton-Robinson (BR) buffer pH 3. Under the optimized experimental conditions, square-wave voltammetry (SWV) and differential pulse voltammetry (DPV) were performed in three measurement modes: selective determination of one analyte in the presence of low concentrations of another one (first and second measurement mode) and the simultaneous determination of both purine derivatives (third measurement mode). Using the suitable values of pulse parameters, the thick-film BDD electrode showed the good linear response in the concentration ranges of (9.2 – 95.0) μM and (4.6 – 95.7) μM for the simultaneous quantification of both compounds by SWV and DPV, respectively. The detection limit was determined to be 6.0 μM and 3.9 μM for UA and 4.6 μM and 2.1 μM for CAF by SWV and DPV, respectively. The selectivity of the proposed sensor was evaluated by the examination of the impact of some inorganic and organic substances, which are commonly present in biological samples, on the current responses of UA and CAF. Finally, the miniaturized thick-film BDD electrode was successfully applied for the electrochemical determination of UA and CAF in human urine and human plasma samples using both pulse techniques with adequate recoveries ranging between 93.7% and 103.3% and without tedious sample pretreatment procedures.

1. Introduction

Purines are compounds which are of vital importance to all living organisms. They are essential for the synthesis of nucleic acids, proteins, other metabolites as well as for energy requiring reactions and cofactors to promote cell survival and proliferation [1]. Caffeine and uric acid are one of the most widely studied purine compounds in clinical trials. Caffeine (CAF) is an example of the commonly used xanthine derivatives in daily human life, which is introduced into the body fluids by consuming tea, coffee, soft and energy drinks and chocolate. It has many important physiological effects, such as stimulation of the central nervous system, diuresis and gastric acid secretion [2]. Uric acid (UA) is the final oxidation (breakdown) product of purine metabolism present in

body fluids (e.g. serum and urine). The normal concentration range of UA in human blood varies from 150 μM to 510 μM [3,4]. Higher than normal levels of UA in the urine often indicate different diseases including mostly hyperuricemia [5,6]. Hence, the quantitative determination of UA levels may be served as a kind of clinically valuable diagnostic indicator which prevents sudden appearance of many diseases [7]. Several epidemiological studies investigated that there is a clear link between CAF-rich beverages consumption and UA concentrations [8]. Some of these studies reported that coffee and tea consumption may affect serum UA levels via various mechanisms including influence on insulin resistance [9–13]. One cross-sectional study revealed a serious inverse association between coffee consumption and UA levels in serum but no association with tea consumption [14].

Furthermore, the another study showed that coffee consumption was correlated with a lower serum UA levels and a lower frequency of hyperuricemia [13] and a decreased risk of gout [15]. Therefore, rapid and simple screening of these compounds in the biological fluids still remains of great importance in clinical analysis for disease diagnosing and further medical treatment. A number of analytical methods have previously been presented for monitoring of purine derivatives in real samples including high-performance liquid chromatography (HPLC) [16,17] and capillary electrophoresis [18]. These methods are sensitive, however most of them are relatively expensive for large scale applications, need elaborate sample preparation, and time-consuming analysis process, which is unfavourable for fast identification and quantitation of adulterations in point-of-care testing or in laboratories with minimal infrastructure.

In recent years, electrochemical sensing has created a revolution in the field of biomedical applications and "fit-for-purpose" clinical diagnostics due to its simplicity, rapid response, high sensitivity and precision. Moreover, these features are accompanied by the possibility of multi-component analysis for real time measurements without analyte derivatization, which is nowadays bringing them to the forefront in the field of instrumental analytical methods. In addition, they do not require highly specialized and expensive laboratory equipment and well-trained operators. They can also be used in complex matrix and non-transparent (dispersed) mediums without further laborious, time-consuming and complicated modifications [19,20].

During the last decade, a few studies reported results on simultaneous electrochemical determination of UA and CAF using chemically modified electrodes based on different modifiers and additional agents such as electrochemically reduced graphene oxide [21], gold nanoparticles and multi-walled carbon nanotubes [22], Fe-doped MgNi$_2$O$_3$ nanoparticles [23], and electropolymerized layer of *p*-aminobenzenesulfonic acid [24]. It is well mentioned here that the use of chemically modified electrodes undoubtedly has huge advantages in terms of sensitivity and selectivity of electrochemical determination, but the preparation of such electrodes often involves lengthy procedures, which can lead to the introduction of undesirable systematic errors eventuating in non-reproducibility of the results.

The advances are being made in this field leading to the development of miniaturized and portable systems, especially electrochemical sensors prepared from alternative and inexpensive materials, often applied for quick on-site analysis [20]. The screen-printing technology is a well-established method to prepare cost-effective sensors, which are disposable in nature and require a reduced volume of the analyte (microlitres) [25–27]. However, it should be underlined that the performance of screen-printed electrodes is greatly influenced by the nature of the working electrode material. The numerous conventional materials such as graphite, conductive polymers, glassy carbon and metals have been utilized for the construction. On the other hand, the usage of robust three-electrode systems based on boron-doped diamond (BDD) working electrode has found to be a strong and unique candidate in last decade due to its wide potential range with the possibilities of electroanalysis at very negative and very positive potentials, low background currents and low adsorption ability, inherent robustness and good biocompatibility with no/negligible effect on human health and environment [28–31].

As for electrochemistry of UA and CAF, we have recently studied the redox behaviour and the options for determination of UA and CAF on bare BDD electrodes, however only individually, without taking into account their mutual presence and influence [7,32]. In this proof-of-concept study, an unmodified miniaturized thick-film BDD electrode was utilized for the first time as a modern and powerful electrochemical platform for the rapid on-site individual and simultaneous determination of selected purines, UA and CAF, with successful analytical validation. The practical feasibility of the suggested sensing platform was demonstrated in the analysis of biological samples such as human urine and human plasma. The portability of the system in tandem with a simple sample pretreatment operation (only centrifugation and/or common dilution in supporting electrolyte) makes the proposed easy-to-use protocol very favourable for rapid point-of-care testing also in laboratories with minimal and/or restricted infrastructure.

2. Experimental

2.1. Apparatus

All voltammetric experiments were carried out using a 910 Mini-potentiostat (Metrohm Autolab B.V., The Netherlands) controlled with PSTAT software. During electrochemical experiments, the miniaturized three-electrode system (purchased from DropSens, Asturias, Spain) situated on ceramic substrate, including the thick-film BDD working electrode (boron doping level of 2500 ppm and inner diameter of 3.6 mm), screen-printed silver pseudoreference electrode and screen-printed carbon auxiliary electrode was exploited. Between individual measurements, the BDD electrochemical sensor was cleaned and pretreated by applying three cyclic voltammetric scans in a potential range from 0 V to +2 V in 0.2 M NaOH at a scan rate of 0.1 V/s with a subsequent rinsing by deionized water. The cleaning procedure was carried out in an independent electrochemical cell. The pH measurements were realized using pHenomenal® pH 1100L meter (VWR, Slovakia) with combined glass-reference electrode.

2.2. Chemicals and solutions

All chemicals and reagents employed in this work were of analytical grade and were obtained from Sigma Aldrich (Slovakia) or Centralchem (Slovakia). The stock solutions of UA and CAF (both of 10 mM) were prepared by dissolving in water, but as the solubility of UA is slightly limited in water, 1 mL of 0.2 M NaOH was added to achieve its complete dissolution. Afterwards, the solutions were quantitatively transferred to a 50 mL volumetric flask and stored in a refrigerator at 6 °C. In the case of CAF, the solution was sufficiently stable for a few months. Regarding the stock solution of UA, the changes in colour and consistency of the solution were gradually noticed after about three weeks, therefore, it had to be prepared more frequently. The working solutions were daily prepared by dilution of the stock solutions to the desired concentration with Britton-Robinson (BR) buffer as a supporting electrolyte. BR buffer in the pH range from 2 to 12 was prepared by mixing of H$_3$BO$_3$, H$_3$PO$_4$, CH$_3$COOH (each of these acids had a final concentration of 0.04 M) and adjusted with 0.2 M NaOH to the required pH value.

2.3. Procedure for preparation of spiked human plasma samples

The commercial human plasma (with 4% trisodium citrate as anticoagulant) was purchased from Sigma Aldrich (Slovakia). Firstly, in order to accomplish protein precipitation in sample, 1 mL of (dried) human plasma was transferred to a centrifuge tube containing 1 mL of deionized water and 1 mL of acetonitrile and placed into an ultrasonic bath for 15 min. Consequently, the mixture was centrifuged for 20 min at 4000 rpm (the precipitate was formed) and the aliquot volume (1 mL) of the obtained supernatant was added to BR buffer pH 3 in the electrochemical cell to the total volume of 10 mL (final dilution factor equaled to 1:20, *v/v*). Finally, the analysis was performed by the standard addition method.

2.4. Procedure for preparation of spiked human urine sample

The urine sample was collected from healthy and non-smoking volunteer on an empty stomach (female, 25 years). These experiments were undertaken in approval with respective law (Parliamentary Act No. 40/1964 Coll. Civil Code as amended) with the informed consent obtained from the volunteer prior to the voltammetric experiments. For the electrochemical measurements, the aliquot volumes of fresh urine (0.2 mL, 0.5 mL and 1.0 mL) were transferred in the electrochemical cell,
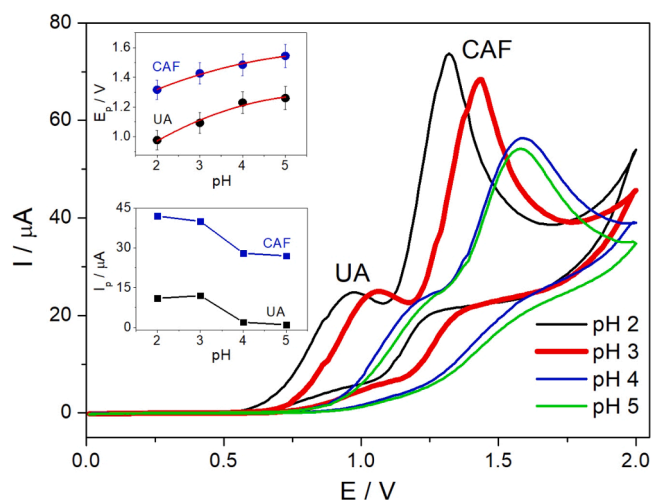
Fig. 1. CV records of 1 mM equimolar mixture of UA and CAF in BR buffer at different pH values between 2 and 5 on the miniaturized thick-film BDD electrode in the potential range from 0 V to + 2 V using the scan rate of 0.1 V/s. Inset: plots of peak potentials (E_p) and peak currents (I_p) vs. pH.

completed with BR buffer (pH 3) to the final volume of 10 mL. The SA method was utilized for the quantification of UA and CAF and the calculation of recovery values.

2.5. Measurement procedures

Cyclic voltammetry (CV) and linear sweep voltammetry (LSV) were employed for the preliminary studies on the electrochemical behaviour of UA and CAF. Square-wave voltammetry (SWV) and differential pulse voltammetry (DPV) were applied for the development of novel electroanalytical protocol for the reliable simultaneous quantification of UA and CAF in biological samples. Under the optimized experimental conditions, the calibration curves were constructed after addition of UA and CAF standard solutions into the electrochemical cell and filled up with supporting electrolyte to 10 mL. All measurements were carried out in triplicate for each concentration at laboratory temperature. The voltammograms obtained after each addition were estimated "as-grown" without using background correction. The results were statistically analyzed by OriginPro 8.0 (OriginLab, USA) and the relevant results
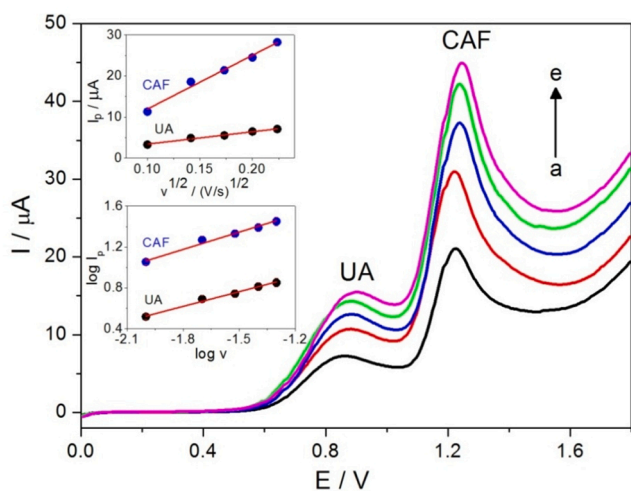

Fig. 2. LSV curves of 1 mM equimolar mixture solution UA and CAF in BR buffer pH 3 on the miniaturized thick-film BDD electrode recorded at different scan rates: a) 0.01 V/s, (b) 0.02 V/s, (c) 0.03 V/s, (d) 0.04 V/s and (e) 0.05 V/s. Insets: the dependences I_p vs. $v^{1/2}$ and log I_p vs. log v.

(slope and intercept) were assessed in a 95% confidence interval. The detection limit (LOD) and quantification limit (LOQ) values were calculated using following equations: LOD = $3 \times s_a/b$; LOQ = $10 \times s_a/b$; where s_a is a standard deviation of intercept, and b is a slope of the particular calibration curve.

3. Results and discussion

3.1. Voltammetric behaviour of UA and CAF on miniaturized thick-film BDD electrode

3.1.1. Effect of pH

The individual electrochemical behaviour of UA and CAF in BR buffer on the BDD electrode has been widely studied in plenty of previous studies including the recent reports of our working group [2,7,32]. Herein, in the proposed work, the early examination was focused on the study of pH effect of supporting electrolyte (BR buffers from pH 2 to 12) on the CV current responses of UA and CAF in their 1 mM individual solutions on the miniaturized thick-film BDD electrode. Fig. S1 and Fig. S2 (Supplementary Material) demonstrably show that the pH of BR buffer quite significantly affects the peak potential and the peak current of both studied analytes. As for UA, the peak performance was similar for pH 2 and 4 (around + 0.95 V and 23 µA). However, as pH increased from 4 to 12, its peak potential shifted towards more positive potential values (from 1.0 V to + 1.3 V) and the background current enhanced. Regarding CAF, the substantial shift of its peak potential towards negative potential values was observed when pH ≥ 4 of BR buffer was used. This fact already predetermined that an acidic environment should be suitable for simultaneous detection of UA and CAF with sufficient peak-to-peak resolution. Furthermore, the representative CV curves of 1 mM equimolar mixture of UA and CAF in BR buffer with pH 2–5, recorded in the potential range from 0 V to + 2 V at a scan rate of 0.1 V/s, are shown in Fig. 1. As can be inferred from these voltammograms, UA and CAF were electrochemically oxidized on the BDD electrode rendering two irreversible oxidation signals at about +(0.9 – 1.25) V for UA and +(1.3 – 1.6) V for CAF depending on pH, respectively. Based on that, the peak-to-peak potential difference between oxidation peaks of analytes (approximately 0.3 V) was evaluated as large enough to ensure simultaneous determination without additional surface modification steps. At higher pH values, the oxidation peak of UA shifted toward more positive potential values (Fig. S1), thus interfering with the CAF oxidation signal. Decreasing the acidity of the analyzed mixture resulted in a decrease of the magnitudes of the peak currents (I_p) for both compounds, indicating that protons have taken part in the electrode reaction processes. In addition, UA oxidation peak practically merged with the CAF signal at pH ≥ 6, demonstrating that an acidic pH environment appeared to be more suitable for the purposes of work. Therefore, pH 3 (red curve in Fig. 1) was selected as suitable due to the highest UA current response and lower background current in comparison with pH 2. However, multi-scan CV recording revealed that a fluctuation of the current response associated with UA causing its partial overlapping with CAF signal (the results are not shown). For this reason, in order to renew the working electrode surface and avoid passivation issues, several cleaning procedures of the miniaturized thick-film BDD electrode were applied involving utilization of CV scans in different environments such

Table 1

Evaluation of SWV and DPV parameters for the simultaneous determination of UA and CAF on the miniaturized thick-film BDD electrode.

Pulse technique	Considered parameter	Studied range	Selected value
SWV	Modulation amplitude (mV)	10–75	75
	Frequency (Hz)	10–40	20
DPV	Modulation amplitude (mV)	10–125	75
	Modulation time (ms)	10–125	25

as BR buffer, H$_2$SO$_4$ and NaOH. It was found that the cycling in 0.2 M NaOH from 0 V to + 2 V (3 cycles at a scan rate of 0.1 V/s) led to the much larger UA peak definition, a steady baseline and an excellent UA and CAF peak-to-peak resolution which as a consequence resulted in higher sensitivity and selectivity.

Though the electrochemical mechanism of UA and CAF is beyond the scope of this work and is documented in many scientific papers [2,7,32], a specific comment can be made. CAF is a weak base with a very low pK_a value (~0.7), which means that nitrogen can only be protonated in very

Fig. 2. It became evident that the oxidation peak currents (I_p) increased gradually and shifted towards more positive potentials with the scan rate (v) from 0.01 V/s to 0.15 V/s for CAF (data not shown) and from 0.01 V/s to 0.05 V/s for UA, confirming the irreversible nature of the electrochemical processes for both compounds. Apart from that, as shown in the first inset of Fig. 2, the linear relationships were obtained by plotting I_p of both UA and CAF against $v^{1/2}$, and can be expressed by the following equations (Eq. (1), Eq. (2)):

$$I_p \ (\mu A) \ = \ (0.40 \ \pm \ 0.30) \ + \ (30.2 \ \pm \ 1.74) \ \times \ v^{1/2} \ \left((V/s)^{1/2} \right) \qquad\qquad R^2 \ = \ 0.9872 \ for \ UA \qquad\qquad (1)$$

$$I_p \ (\mu A) \ = \ (1.13 \ \pm \ 1.53) \ + \ (131.0 \ \pm \ 8.84) \ \times \ v^{1/2} \ \left((V/s)^{1/2} \right) \qquad\qquad R^2 \ = \ 0.9824 \ for \ CAF \qquad\qquad (2)$$

strong acidic solutions [32,33]. By the pH increasing, the unprotonated free base form of CAF (neutral species) predominates in the supporting electrolyte [33]. This can be explanation why no significant shift in the peak potentials (E_p) of CAF was registered with the increasing of pH from 4 to 5. However, as can be seen in Fig. 1, in the pH range from 2 to 3 for CAF, E_p values shifted towards more positive values with the increasing of pH (first inset of Fig. 1), demonstrating that protons are consumed during the reaction. Hence, it can be suggested that the overall process of CAF oxidation involves the loss of two electrons together with the addition of an H$^+$ and OH$^-$ onto the double bond. This may be followed by the chemical reaction in solution resulting in a loss

In addition, the linear dependences between log I_p and log v (second inset of Fig. 2) with the particular slope values of 0.48 and 0.56 for UA and CAF, respectively, which were very similar to the theoretical value of 0.5, clearly implied a diffusion-controlled electrochemical process for both compounds on the BDD electrode. The equations acquired from these linear relations were as follow (Eq. (3), Eq. (4)):

$$log I_p \ = \ (1.48 \ \pm \ 0.09) \ + \ (0.48 \ \pm \ 0.06) \ \times \ log v \qquad\qquad R^2 \ = \ 0.9895 \ for \ UA \qquad\qquad (3)$$

$$log I_p \ = \ (2.19 \ \pm \ 0.10) \ + \ (0.56 \ \pm \ 0.06) \ \times \ log v \qquad\qquad R^2 \ = \ 0.9816 \ for \ CAF \qquad\qquad (4)$$

of two more electrons and four protons. These facts are in good agreement with data found on a glassy carbon electrode modified with an electropolymerized film of *p*-aminobenzenesulfonic acid [24]. As for UA, the mechanism of electrochemical oxidation is not so clear; E_p variation towards more positive values (Fig. S1) can be also explained by impact of the electrochemical oxidation of CAF which results in more intense peak currents and dragging on it, but for more close information additional studies are necessary.

3.1.2. Effect of scan rate

The nature of the electrode reactions of UA and CAF on the miniaturized thick-film BDD electrode was explored considering the impact of scan rate (v) in the range of (0.01 – 0.05) V/s on the peak currents of both analytes. Following the findings that UA and CAF behave as electrochemically irreversible systems, linear sweep voltammetry (LSV) instead of CV was utilized. The LSV records of 1 mM equimolar mixture of UA and CAF in BR buffer pH 3 at various scan rates are presented in

However, it should be stated that after exceeding the scan rate of 0.05 V/s, the linearity was disrupted and the current response of UA did not increase with growing of scan rate in the validity of Randles-Sevcik equation. It could be explained by the fact that at higher scan rates there was also a partial adsorption of the analytes and/or products of the competing electrochemical reactions of UA and CAF on the miniaturized thick-film BDD electrode.

3.2. Analytical performance

3.2.1. Optimization of differential pulse and square-wave voltammetric parameters

In order to achieve the sufficient sensitivity and selectivity, instrumental parameters such as modulation amplitude and modulation time for differential pulse voltammetry (DPV) and modulation amplitude and
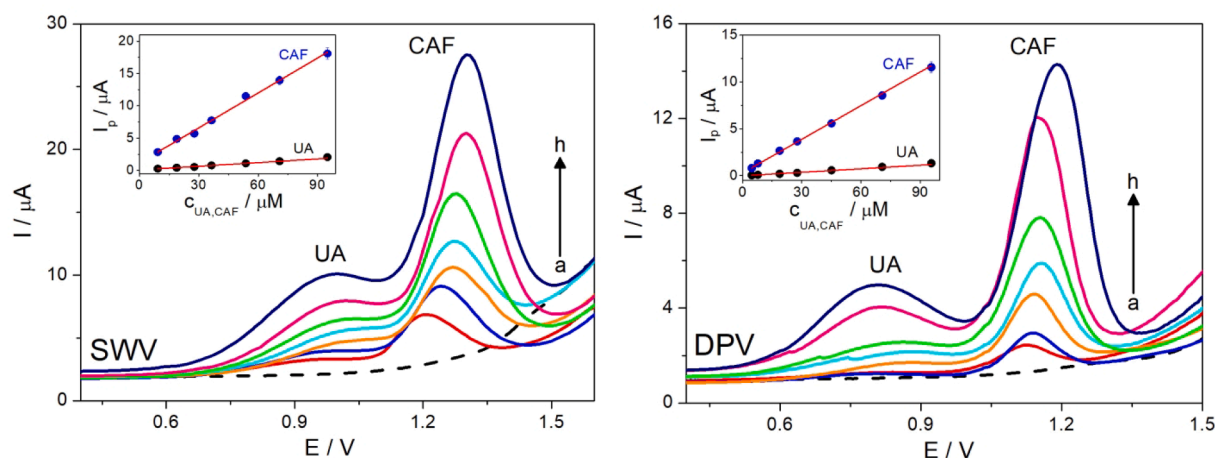
Fig. 3. SWV and DPV records of mixture solutions of UA and CAF obtained at their equal concentrations in BR buffer pH 3 (a → h) on the miniaturized thick-film BDD electrode. SWV: (a) 0 μM (blank), (b) 9.17 μM, (c) 18.9 μM, (d) 27.7 μM, (e) 36.4 μM, (f) 53.7 μM, (g) 70.8 μM and (h) 95.0 μM. DPV: (a) 0 μM (blank), (b) 4.63 μM, (c) 7.76 μM, (d) 18.8 μM, (e) 27.7 μM, (f) 45.1 μM, (g) 70.8 μM and (h) 95.7 μM. The corresponding calibration curves are displayed in the insets.

frequency for square-wave voltammetry (SWV) were submitted for evaluation (see summary in Table 1).

When selecting the appropriate conditions for the SWV, the modulation amplitude was varied in the range from 10 mV to 125 mV while the frequency was constant with a default value of 10 Hz. As shown in Fig. S3 (Supplementary Material), I_p of UA and CAF increased progressively upon enhancement of modulation amplitude until 75 mV, whereas at its higher values (the results not shown) the background current increased sharply, impairing the signal-to-noise (S/N) ratio. Comparing the shape and current responses of UA and CAF, modulation amplitude of 75 mV was selected as the most appropriate. Regarding the frequency explored in the range of (10 – 40) Hz (with the modulation amplitude fixed at 10 mV), its enhancement was accompanied by the serious increasing of background current (from 0.3 μA to 2 μA) and widening of both peaks as demonstrated in the inset of Fig. S3.

As for optimization of DPV instrumental parameters, a variation of modulation amplitude up to 125 mV with the modulation time fixed at 10 ms brought rise of both signal intensities (Fig. S4 in Supplementary Material) arriving to plateau up to 75 mV. Hence, 75 mV was set as the compromise since this value allowed satisfactory resolution and excellent current response. On the other hand, as shown in the inset of Fig. S4, the increasing of modulation time in the range of (10 – 125) ms (with modulation amplitude fixed at 10 mV) caused the rapid decline of background current and as a consequence increase in S/N ratio. Therefore, the modulation amplitude of 25 ms was found to be suitable for all subsequent experiments.

Table 2

Analytical parameters for voltammetric determination of UA and CAF obtained on the miniaturized thick-film BDD electrode for 1st and 2nd mode.

Analytical parameter	First measurement mode		Second measurement mode	
	Pulse voltammetric technique			
	SWV	DPV	SWV	DPV
	UA		CAF	
Intercept (μA)	−0.7053 ± 0.1132	−0.1914 ± 0.0235	−1.6413 ± 0.2846	−0.1742 ± 0.1573
Slope (μA/μM)	0.0928 ± 0.0023	0.0327 ± 0.0005	0.3050 ± 0.0060	0.1882 ± 0.0033
Linear range (μM)	7.4 – 90.7	5.7 – 90.7	6.5 – 90.6	2.0 – 100
R^2	0.9956	0.9983	0.9973	0.9972
LOD (μM)	3.7	2.2	2.8	2.5
LOQ (μM)	12.2	7.2	9.3	8.4

Table 3

Analytical parameters for voltammetric determination of UA and CAF obtained on the miniaturized thick-film BDD electrode for 3rd mode.

Analytical parameter	Third measurement mode: simultaneous determination of UA and CAF			
	Pulse voltammetric technique			
	SWV		DPV	
	UA	CAF	UA	CAF
Intercept (μA)	−0.0344 ± 0.0414	1.2681 ± 0.2770	−0.0525 ± 0.0183	0.4515 ± 0.0793
Slope (μA/μM)	0.0207 ± 0.0008	0.1793 ± 0.0052	0.0141 ± 0.0004	0.1126 ± 0.0016
Linear range (μM)	9.2 – 95.0	9.2 – 95.0	4.6 – 95.7	4.6 – 95.7
R^2	0.9914	0.9948	0.9959	0.9988
LOD (μM)	6.0	4.6	3.9	2.1
LOQ (μM)	20.0	15.4	12.9	7.0
Repeatability (%) *	4.6	3.2	4.4	3.1

*RSD for 7 replicate DPV or SWV measurements for 15 μM mixture solution of UA and CAF.

3.2.2. Analytical characteristics

Under optimized experimental conditions, the ability of miniaturized thick-film BDD electrode for individual and simultaneous determination of UA and CAF was tested in three different modes by both pulse techniques. The first mode was realized by gradually increasing of the UA concentration (c_{UA}), while the CAF concentration (c_{CAF}) was kept at a definite value of 15 μM (Fig. S5A and Fig. S5B in Supplementary Material). The second mode of determination consisted in maintaining the constant c_{UA} at a value of 10 μM and varying in c_{CAF} (Fig. S5C and Fig. S5D in Supplementary Material). In the third mode, the calibration curves were constructed for simultaneous enhancement of the concentration of both analytes (Fig. 3). As depicted in the insets of Fig. S5A-D, the oxidation signals of UA and CAF increased upon adding one analyte, whereas the small decrease in the current response of substance with a constant concentration took place, indicating that there was minor interference in the determination of UA and CAF owing to their coexistence. The BDD electrode exhibited wide linear concentration ranges with the determination coefficients above 0.995 for all three modes. By comparing the sensitivities of both pulse techniques in first two modes through the evaluation of slope values, it should be underlined that the slope value achieved in first measurement mode by DPV was roughly 3-fold lower when compared to SWV (0.0327 against 0.0928 μA/μM).

Similarly in the second mode, SWV appeared to be more sensitive (0.3050 against 0.1882 µA/µM). In spite of these facts, the comparable sensitivity values were achieved in third mode for both techniques. Hence, calculated LODs for UA determination in the presence of fixed concentration of CAF were 2.2 µM and 3.7 µM for DPV and SWV, respectively. For CAF determination in the presence of constant UA concentration, LODs were very similar of 2.5 µM and 2.8 µM for DPV and SWV, respectively. On the other hand, when comparing the result for simultaneous determination in third mode, it should be noted that the BDD electrode showed approximately 2-fold higher LODs for UA and CAF when compared to first or second modes. An explanation can be found in above-mentioned interference of analytes with mutually influencing the electrochemical characteristics. The overall statistical evaluation for the presented electrochemical sensing platform and the main analytical parameters are summarized in Table 2 and Table 3.

The intra-day repeatability was investigated by 7 successive replicate measurements for 15 µM mixture solution of UA and CAF. The relative standard deviation (RSD) values in peak currents were found to be 4.6% and 4.4% for UA as well as 3.2% and 3.1% for CAF using SWV and DPV, respectively. On the basis of these values it can be concluded that the developed advanced voltammetric protocol is adequately precise.

3.2.3. Interferences

The selectivity of the developed electroanalytical method was evaluated by the examination of the ability of the miniaturized thick-film BDD electrode to determine UA and CAF in the presence of substances that are commonly present in biological samples (urine, plasma) without any significant interference from them. The potential interfering agents were artificially added to a 10 µM mixture solution of UA and CAF, as concentration ratios (UA/CAF/interferent(s), *v/v/v*): 1/1/1, 1/1/10, 1/1/20 and 1/1/50), and DP voltammograms were recorded. The tolerance limit was defined as the maximum concentration of the foreign substances, which caused an approximately ± 5% relative error in the determination of both compounds. The results revealed that 50-fold excess of inorganic ions such as K^+, Na^+, Mg^{2+}, Ca^{2+}, Cl^- and SO_4^{2-} did not have significant impact on the simultaneous determination of UA and CAF. Ascorbic acid (AA) and dopamine (DOP) are one of the most common organic molecules co-existing in body fluids in relatively considerable concentrations. The normal AA range in urine in a healthy individual is stated of (0.029 – 0.074) mM [34], while normal range of DOP is (0.3 – 3.1) µM [35]. Thus, the investigation of the interference that may result from the presence of a wide concentration range of AA and DOP is of great relevance (Fig. S6 in Supplementary Material). Since both AA and DOP undergo electrochemical oxidation at approximately the same potentials as UA on bare carbon-based electrodes, the significant increase in UA peak current (about 33%) was noticed already in equimolar AA concentration ratio, while the oxidation signal of CAF was almost not affected (the change is lower than 2%). In the case of the presence of 10-fold higher AA concentrations, the gradual changes in CAF signal were also registered, leading to complete overlapping of two peaks in the presence of 50-fold excess of AA. On the contrary, when DOP was present in equal concentration, no obvious interference (the change is lower than 4%) was observed for simultaneous determination of UA and CAF. With the addition of higher DOP concentration, the UA signal became more occluded by the DOP signal and eventually completely disappeared. But as it was mentioned earlier the ordinary DOP levels are much lower as tested ones. Due to a wide variety of functions of vitamins in the body, the interfering effect of water-soluble vitamin of B group pyridoxine (PYR) was also explored in different ratios. Since PYR is structurally very similar to CAF, oxidation signals of PYR appeared at the same potential as CAF (near + 1.3 V). The results in Fig. S6 proved that PYR showed no fundamental impact on the electrochemical oxidation of UA and CAF at equal concentration levels. But beginning with 10-fold excess, the signal changes of both compounds were above the tolerance limit. In regards to sugars, the voltammetric profiles of both analytes were softly influenced by the presence of
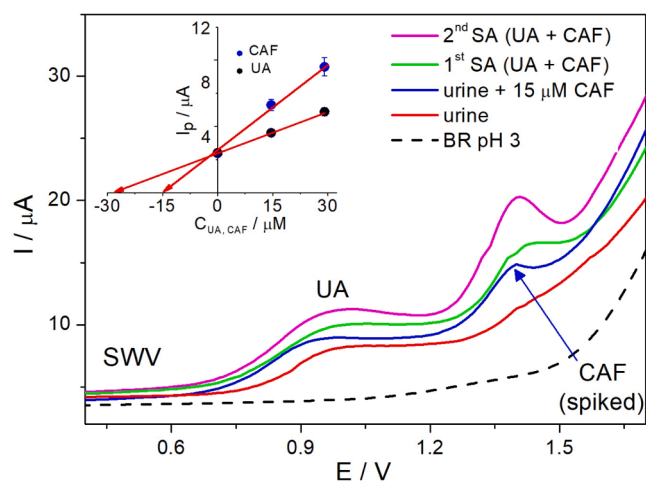

Fig. 4. SWV records of the simultaneous determination of UA and CAF in the presence of spiked concentration of 15 µM CAF in human urine sample (0.5 mL fresh urine completed to 10 mL with BR buffer pH 3) on the miniaturized thick-film BDD electrode. The corresponding standard additions (SA) of UA: 150 µL and 300 µL (c_{UA} = 1 mM) and CAF: 150 µL and 300 µL (c_{CAF} = 1 mM). The SWV parameters: amplitude of 75 mV, frequency of 20 Hz and scan rate of 0.25 V/s. The graphical evaluation of quantification by standard addition method is appended in the inset.

Table 4
The results of analysis of human urine samples using the proposed electrochemical sensing platform.

Analyte	Volume of added urine (mL)	Spiked (µM)	Determined amount (µM)		Recovery (%)	
			DPV	SWV	DPV	SWV
The UA quantification in the presence of fixed CAF concentration						
UA	1.0	–	552 ± 20	547 ± 23	–	–
	0.5	–	555 ± 24	550 ± 18	–	–
	0.2	–	554 ± 17	540 ± 25	–	–
The CAF quantification in the presence of fixed UA concentration						
CAF	1.0	15.0	14.1 ± 0.9	14.7 ± 0.4	93.7	98.0
The simultaneous determination of UA and CAF						
UA	0.5	–	554 ± 14	550 ± 12	–	–
CAF		15.0	15.5 ± 0.7	15.2 ± 0.3	103.3	101.1

glucose and/or sucrose in 50-fold excess. Based on the obtained results, it can be concluded that the direct utilization of the miniaturized thick-film BDD electrode for the simultaneous determination of UA and CAF could be slightly limited in certain concentration levels of the aforementioned interfering substances. On the other hand, the concentration levels of interfering agents such as DOP and AA in healthy individuals are 1–3 orders of magnitude lower than UA and comparable to CAF.

3.3. Analysis of human biological fluids

The functionality of the miniaturized thick-film BDD electrode for the determination of UA and CAF in human biological fluids such as urine and plasma was evaluated using pulse techniques. To perform it, the samples were pre-treated as described in Sections 2.3 and 2.4. The voltammograms of 10-fold diluted human urine displayed one signal peak ($E_{p1} \approx +0.9$ V), that can be due to the electrochemical oxidation of UA on the BDD electrode while the oxidation signal of CAF was not registered. Subsequently, we realized that the CAF content in particular
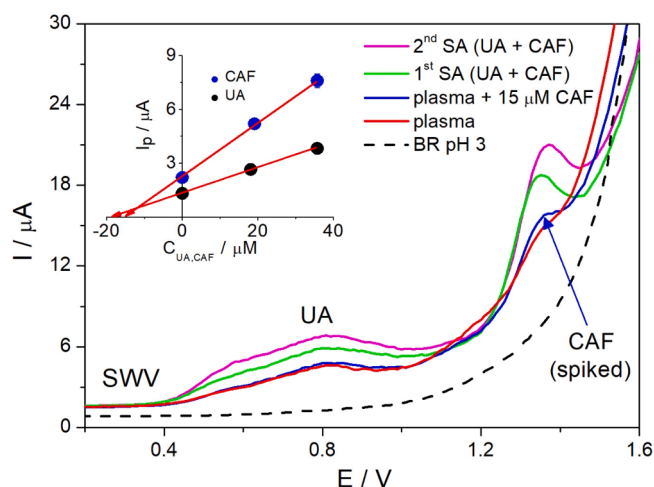
Fig. 5. SWV records of the simultaneous determination of UA and CAF in the presence of spiked concentration of 15 μM CAF in commercially-available human plasma (1 mL supernatant completed to 10 mL with BR buffer pH 3) on the miniaturized thick-film BDD electrode. The corresponding standard additions (SA) of UA: 200 μL and 400 μL (c_{UA} = 1 mM) and CAF: 200 μL and 400 μL (c_{CAF} = 1 mM). The SWV parameters: amplitude of 75 mV, frequency of 20 Hz and scan rate of 0.25 V/s. The graphical evaluation of quantification by standard addition method is appended in the inset.

Table 5
The results of simultaneous determination of UA and CAF in human plasma sample (dilution factor of 1:20, *v/v*) using the proposed electrochemical sensing platform.

Analyte	Spiked (μM)	Determined amount (μM)		Recovery (%)	
		DPV	SWV	DPV	SWV
UA	–	422 ± 18	385 ± 17	–	–
CAF	15.0	14.4 ± 0.6	15.2 ± 0.5	96.1	101.3

human urine sample is very low (below LOD) and completely out of the dynamic concentration range of the calibration curve. Consequently, the sample was spiked with the low concentration of CAF. To confirm the presence of UA and to determine its concentration in the presence of 15 μM CAF, the different standard additions of UA were injected into diluted urine sample, while the concentration of CAF was unchangeable of 15 μM during the analysis. It was found that the well-shaped oxidation peak at + 0.9 V was appeared to be sensitive to each standard addition and increased proportionally with their concentrations within the corresponding linear ranges (Fig. 4). Based on the obtained results it was found that the tested urine sample (e.g. 0.5 mL fresh urine, see Table 4) contained UA in concentration levels of (555 ± 24) μM by DPV and (550 ± 18) μM by SWV, showing a fair agreement with the slightly higher UA concentration when compared to normal UA levels (150 μM – 510 μM) [3,4]. The corresponding SW voltammograms for the determination of UA in the presence of CAF are illustrated in Fig. S7 (Supplementary Material). In next step, the possibility for determination of CAF in the presence of UA was tested; the urine sample was spiked by 15 μM CAF and analyzed using the multiple standard addition method (Fig. S8 in Supplementary Material). In the final step, this electroanalytical protocol was also utilized for the simultaneous determination of UA and CAF in spiked urine sample (Fig. 4). As can be seen in Table 4, the recovery values obtained by both pulse techniques in all three modes with the BDD electrode were satisfactory (in the range from 93.7% to 103.3% for both pulse techniques) indicating high accuracy of the herein proposed electrochemical sensing platform.

Regarding the commercially-available human plasma sample, in order to reduce the matrix effect, the analysis was carried out by the

standard addition method. The DPV and SWV records indicated the presence of one "ill-defined" oxidation peak at around + 0.85 V which can be due to the electrochemical oxidation of UA (red curve for SWV in Fig. 5). At the same time, no voltammetric signal at higher positive potentials (>1 V) corresponding to the oxidation of CAF was observed clearly demonstrating the absence of this compound in origin human plasma sample. To confirm the verification of the proposed sensor for human plasma analysis, the known amount of CAF (blue curve for SWV in Fig. 5) was injected to the diluted plasma sample (1:20, *v/v*) in electrochemical cell and then spiked with two standard additions of 200 μL of UA and CAF stock solutions (each 1 mM) and then analyzed in triplicate. The determination of UA and CAF in human plasma by the standard addition method is illustrated in Fig. 5. The concentrations of UA in plasma samples were found to be (385 ± 17) μM for SWV and (422 ± 18) μM for DPV, which are in the common range for healthy people [3,4]. In addition, CAF values found presented the good agreement with CAF spiked concentrations, which were considered as the reference ones. The recovery values were 96.1% and 101.3% (Table 5) for DPV and SWV, respectively, which validate the versatility of the miniaturized thick-film BDD electrode in combination with pulse techniques for reliable human plasma analysis.

3.4. Comparison with other voltammetric methods

Firstly, it is worth mentioning that despite the fact that UA and CAF are electrochemically active compounds, no voltammetric study in the scientific literature has been reported to the simultaneous determination of UA and CAF using bare (unmodified) working electrode materials. It can be explained by the fact that the oxygen evolution reaction on the bare electrodes interferes with the electrode reaction of CAF at enough high positive potentials [2]; or another logical explanation can be found in low resistance of conventional electrodes to fouling and deactivation caused by UA oxidation. In all four previously reported works, the special attention has been paid to the strategies using modification steps within the sensor preparation before the determination. For instance, *Raj et al.* presented the simultaneous determination of UA, xanthine (XN), hypoxanthine (HXN) and CAF in human blood serum and urine samples using electrochemically reduced graphene oxide (ERGO) modified electrode. ERGO modified electrode not only greatly enhanced the current responses of the four purine derivatives, but also shifted their oxidation potentials towards less positive potentials in contrast to bare GCE [21]. Further, GCE chemically modified with an electropolymerized layer of *p*-aminobenzenesulfonic acid (*p*-ABSA) has been developed to determine XN, theophylline (TP) and CAF simultaneously together with UA [24]. In another work, a thiol-functionalized sol–gel-based carbon ceramic electrode (CCE) was constructed. The CCE was further modified by incorporation of gold nanoparticles (AuNP) in the thiol-functionalized ceramic matrix as well as immobilization of multi-walled carbon nanotubes (MWCNT) within the pores of this ceramic sol–gel. It was noted that both modifiers acted as hot spots that could facilitate the electron transfer and as a result enhanced the sensing capabilities. This sensor allowed the simultaneous detection of UA, XN and CAF in both human serum and urine samples with sufficient recovery values [22]. Recently, *Reddy et al.* developed a novel electrochemical sensor based on Fe-doped $MgNi_2O_3$ nanoparticles modified GCE for simultaneous determination of DOP, UA, nicotine (NIC) and CAF with the lowest LOD values for UA (0.104 μM) and CAF (0.276 μM) [23]. By comparing the analytical performance of the above-mentioned methods with our developed bare electrochemical sensing platform (Table S1 in Supplementary Material) it should be underlined that linear concentration ranges obtained using BDD electrode is in more cases comparable to those acquired by chemically modified electrodes. As for sensitivity, it can be seen that all reported papers reveal higher sensitivity in terms of LODs. Nevertheless, it should be underlined that the preparation of chemically modified electrodes is often time-consuming process, requiring various complicated steps, which is unfavourable for fast

routine analysis. Taking all above mentioned aspects into account, it can be concluded that miniaturized thick-film BDD electrode presents several comfortable facilities in this issue such as simplicity, low cost, long-term stability accompanied by high sensitivity without any chemical modification. Besides, it can be successfully utilized as an alternative tool to chemically modified electrodes in on-site investigations or point-of-care testing.

4. Conclusions

As far as we know, previously published papers dealing with voltammetric determination of purine derivatives UA and CAF are mostly focused on the application of chemically modified electrodes. In this study, for the first time, the bare (unmodified) electrochemical sensor based on a miniaturized BDD electrode has been introduced within the modern and powerful electrochemical sensing platform for the simultaneous determination of two purine derivatives as well as for the sufficiently selective determination of one compound in the presence of low concentrations of other one. The obtained results revealed that under the optimized experimental conditions the sufficient resolution between UA and CAF oxidation peak potentials (approximately 0.3 V) could be achieved on the bare miniaturized thick-film BDD electrode without any modification steps. Taking into consideration the normal concentration levels of UA (150 μM – 510 μM) and CAF (1 μM – 20 μM) in complex biological matrices and the sufficiently low LODs (~2 μM – 6 μM) achieved in this work, the miniaturized thick-film BDD electrode is able to provide an effective electrochemical sensing platform for recognizing and reliable determination of UA and CAF in urine and plasma with adequate recovery values. In addition, it should be underlined that the further advantages of the proposed sensor is its high accuracy, reproducibility, simplicity and portability which is very promising for quick quantification in point-of-care testing or in laboratories with minimal and/or restricted infrastructure and without tedious sample pretreatment procedures.

CRediT authorship contribution statement

Olha Sarakhman: Writing – original draft, Supervision, Formal analysis, Investigation, Resources, Data curation, Visualization. **Alžbeta Benková:** Methodology, Validation, Formal analysis, Investigation, Data curation, Visualization. **Ľubomír Švorc:** Conceptualization, Supervision, Writing – review & editing, Paper administration, Funding acquisition.

Declaration of Competing Interest

The authors declare that they have no known competing financial interests or personal relationships that could have appeared to influence the work reported in this paper.

Acknowledgement

Appendix A. Supplementary data

Supplementary data to this article can be found online at https://doi.org/10.1016/j.microc.2021.107132.

References

[1] J. Yin, W. Ren, X. Huang, J. Deng, T. Li, Y. Yin, Potential mechanisms connecting purine metabolism and cancer therapy, Front. Immunol. 9 (2018) 1697–1705.

[2] Ľ. Švorc, Determination of caffeine: A comprehensive review on electrochemical methods, Int. J. Electrochem. Sci. 8 (2013) 5755–5773.

[3] J. Maiuolo, F. Oppedisano, S. Gratteri, C. Muscoli, V. Mollace, Regulation of uric acid metabolism and excretion, Int. J. Cardiol. 213 (2016) 8–14.

[4] H.H. Hamzah, Z.M. Zain, N.L.W. Musa, Y.-C. Lin, E. Trimbee, Spectrophotometric determination of uric acid in urine based-enzymatic method uricase with 4-Aminodiphenylamine diazonium sulfate (Variamine blue RT salt), J. Anal. Bioanal. Tech. S 7 (2013) 1–6.

[5] M.R. Wiederkehr, O.W. Moe, Uric acid nephrolithiasis: A systemic metabolic disorder, Clin. Rev. Bone Miner. Metab. 9 (3-4) (2011) 207–217.

[6] N. Cai, Lu.u Tan, Y. Li, T. Xia, T. Hu, X. Su, Biosensing platform for the detection of uric acid based on graphene quantum dots and G-quadruplex/hemin DNAzyme, Anal. Chim. Acta 965 (2017) 96–102.

[7] K. Cinková, K. Kianičková, D.M. Stanković, M. Vojs, M. Marton, Ľ. Švorc, The doping level of boron-doped diamond electrodes affects the voltammetric sensing of uric acid, Anal. Methods 10 (2018) 991–996.

[8] H.K. Choi, G. Curhan, Coffee consumption and risk of incident gout in women: the nurses' health study, Am. J. Clin. Nutr. 92 (4) (2010) 922–927.

[9] H.J. Petrie, S.E. Chown, L.M. Belfie, A.M. Duncan, D.H. McLaren, J.A. Conquer, T. E. Graham, Caffeine ingestion increases the insulin response to an oral-glucose-tolerance test in obese men before and after weight loss, Am. J. Clin. Nutr. 80 (1) (2004) 22–28.

[10] T. Wu, W.C. Willett, S.E. Hankinson, E. Giovannucci, Caffeinated coffee, decaffeinated coffee, and caffeine in relation to plasma C-peptide levels, a marker of insulin secretion, in U.S. women, Diabetes Care 28 (2005) 1390–1396.

[11] R.M. Van Da, F.B. Hu, Coffee consumption and risk of type 2 diabetes: A systematic review, Clin. Corner 294 (2005) 97–104.

[12] E. Salazar-Martinez, W.C. Willett, A. Ascherio, J.E. Manson, M.F. Leitzmann, M. J. Stampfer, F.B. Hu, Coffee consumption and risk for type 2 diabetes mellitus, Ann. Intern. Med. 140 (1) (2004) 1, https://doi.org/10.7326/0003-4819-140-1-200401060-00005.

[13] H.K. Choi, G. Curhan, Coffee, tea, and caffeine consumption and serum uric acid level: the third national ealth and nutrition examination survey, Arthritis Care Res. 57 (2007) 816–882.

[14] C. Kiyohara, S. Kono, S. Honjo, I. Todoroki, Y. Sakurai, M. Nishiwaki, H. Hamada, H. Nishikawa, H. Koga, S. Ogawa, K. Nakagawa, Inverse association between coffee drinking and serum uric acid concentrations in middle-aged Japanese males, Br. J. Nutr. 82 (2) (1999) 125–130.

[15] K.Y. Park, H.J. Kim, H.S. Ahn, S.H. Kim, E.J. Park, S.-Y. Yim, J.-B. Jun, Effects of coffee consumption on serum uric acid: Systematic review and meta-analysis, Semin Arthritis Rheum. 45 (5) (2016) 580–586.

[16] K. Safranow, Z. Machoy, K. Ciechanowski, Analysis of purines in urinary calculi by high-performance liquid chromatography, Anal. Biochem. 286 (2) (2000) 224–230.

[17] N. Wijemanne, P. Soysa, S. Wijesundara, H. Perera, Development and validation of a simple high performance liquid chromatography/UV method for simultaneous determination of urinary uric acid, hypoxanthine, and creatinine in human urine, Int. J. Anal. Chem. 2018 (2018) 1–6.

[18] P. Wang, J. Ren, Separation of purine and pyrimidine bases by capillary electrophoresis using β-cyclodextrin as an additive, J. Pharm. Biomed. Anal. 34 (2) (2004) 277–283.

[19] I. Jeerapan, S. Poorahong, Review-flexible and stretchable electrochemical sensing systems: materials, energy sources, and integrations, J. Electrochem. Soc. 167 (2020), 037573.

[20] M. Mathew, S. Radhakrishnan, A. Vaidyanathan, B. Chakraborty, C.S. Rout, Flexible and wearable electrochemical biosensors based on two-dimensional materials: recent developments, Anal. Bioanal. Chem. 413 (3) (2021) 727–762.

[21] M.A. Raj, S.A. John, Simultaneous determination of uric acid, xanthine, hypoxanthine and caffeine in human blood serum and urine samples using electrochemically reduced graphene oxide modified electrode, Anal. Chim. Acta 771 (2013) 14–20.

[22] C. Ferrag, M. Noroozifar, K. Kerman, Thiol functionalized carbon ceramic electrode modified with multi-walled carbon nanotubes and gold nanoparticles for simultaneous determination of purine derivatives, Mater. Sci. Eng. C 110 (2020), 110568.

[23] S.L. Reddy, C. Arul, L. Zhaoqi, N. Lavanya, C. Sekar, A novel electrochemical sensor based on Fe-doped $MgNi_2O_3$ nanoparticles for simultaneous determination of dopamine, uric acid, nicotine and caffeine over very wide linear ranges, J. Electroanal. Chem. 878 (2020), 114648.

[24] S. Jesny, K. GirishKumar, Non-enzymatic electrochemical sensor for the simultaneous determination of xanthine, its methyl derivatives theophylline and caffeine as well as its metabolite uric acid, Electroanalysis 29 (7) (2017) 1828–1837.

[25] Z. Taleat, A. Khoshroo, M. Mazloum-Ardakani, Screen-printed electrodes for biosensing: a review (2008–2013), Microchim. Acta 181 (9-10) (2014) 865–891.

[26] F. Arduini, L. Micheli, D. Moscone, G. Palleschi, S. Piermarini, F. Ricci, G. Volpe, Electrochemical biosensors based on nanomodified screen-printed electrodes: recent applications in clinical analysis, TrAC -, Trends Anal. Chem. 79 (2016) 114–126.

[27] A. Hayat, J. Marty, Disposable screen printed electrochemical sensors: Tools for environmental monitoring, Sensors (Switzerland) 14 (6) (2014) 10432–10453.

[28] O. Sarakhman, Ľ. Švorc, A review on recent advances in the applications of boron-doped diamond electrochemical sensors in food analysis, Crit. Rev. Anal. Chem. (2021) In press, DOI: 10.1080/10408347.2020.1828028.

[29] J.V. Macpherson, A practical guide to using boron doped diamond in electrochemical research, Phys. Chem. Chem. Phys. 17 (5) (2015) 2935–2949.

[30] K. Muzyka, J. Sun, T.H. Fereja, Y. Lan, W. Zhang, G. Xu, Boron-doped diamond: Current progress and challenges in view of electroanalytical applications, Anal. Methods 11 (2019) 397–414.

[31] M. Yence, A. Cetinkaya, G. Ozcelikay, S. I. Kaya, S. A. Ozkan, Boron-doped diamond electrodes: Recent developments and advances in view of electrochemical drug sensors, Crit. Rev. Anal. Chem. (2021) In press, DOI: 10.1080/10408347.2020.1863769.

[32] L. Švorc, P. Tomčík, J. Svítková, M. Rievaj, D. Bustin, Voltammetric determination of caffeine in beverage samples on bare boron-doped diamond electrode, Food Chem. 135 (3) (2012) 1198–1204.

[33] H.S. Ali, A.A. Abdullah, P.T. Pınar, Y. Yardım, Z. Şentürk, Simultaneous voltammetric determination of vanillin and caffeine in food products using an anodically pretreated boron-doped diamond electrode: Its comparison with HPLC-DAD, Talanta 170 (2017) 384–391.

[34] S. Wu, T. Sun, H. Wang, Z. Fan, L. Li, B. Fan, L. Liu, J. Ma, Z. Tong, A sandwich-structured, layered CoTMPyP/$Sr_2Nb_3O_{10}$ nanocomposite for simultaneous voltammetric determination of dopamine and ascorbic acid, J. Electroanal. Chem. 873 (2020), 114403.

[35] S. Dalirirad, A.J. Steckl, Lateral flow assay using aptamer-based sensing for on-site detection of dopamine in urine, Anal. Biochem. 596 (2020), 113637.